Adsorption (2010) 16: 185–195
DOI 10.1007/s10450-010-9221-6

# Evidences for the relationship between surface structure and reactivity of goethite nanoparticles based on advanced molecular-probe methods

**Stéphane Stevanovic · Mouhamad AliAhmad · Angelina Razafitianamaharavo · Frédéric Villiéras · Barrès Odile · Bénédicte Prélot · Jerzy Zajac · Jean-Marc Douillard · Corinne Chanéac**

Received: 29 January 2010 / Accepted: 28 May 2010 / Published online: 22 June 2010


**Abstract** Surface properties of two goethites have been studied in order to compare the amount of acid surface sites and their distribution over the various surface domains. For this purpose, ammonia, pyridine and nitrogen were used as basic molecular probes. Calorimetry measurements of ammonia adsorption provided the image of the average surface acidity being moderate. This conclusion was supported by the moderate resistance of the adsorbed pyridine molecules to degassing conditions. Adsorption and desorption of pyridine prior to gaseous nitrogen adsorption resulting in masking/unmasking of acid surface sites on the goethite surface allowed confirmation of the acid character of the specific adsorption sites characterized by the high-energy adsorption of electron-donating molecular nitrogen. The amount of acid sites probed by nitrogen and ammonia were of the same order of magnitude but systematically higher for ammonia. The subsequent analysis of the argon and nitrogen derivatives of first-layer adsorption isotherm led to determine the distribution of {101} and {121} crystallographic faces and discuss the location of acid sites on these surface domains.

S. Stevanovic · A. Razafitianamaharavo · F. Villiéras (✉) · B. Odile
Laboratoire Environnement et Minéralurgie, Université de Lorraine-CNRS, UMR 7569 LEM, ENSG, B.P. 40, 54501 Vandoeuvre-les-Nancy cedex, France
e-mail: frederic.villieras@ensg.inpl-nancy.fr

M. AliAhmad · B. Prélot · J. Zajac · J.-M. Douillard
Institut Charles Gerhardt, UMR-5253 CNRS-UM2-ENSCM-UM1, Agrégats, Interfaces, Matériaux pour l'Energie, C.C. 1502 Place Eugène Bataillon, 34095 Montpellier cedex 5, France

C. Chanéac
Laboratoire de Chimie de la Matière Condensée de Paris, UPMC, CNRS, UMR 7574, LCMC Paris, 75252 Paris, France

**Keywords** Goethites · Ammonia · Pyridine · Nitrogen adsorption · Acid sites

## 1 Introduction

Since nanometer-scale solid particles may exhibit size-related properties that differ significantly from those observed in fine particles or monoliths (Ying 2001), they are nowadays of great scientific interest in materials science as constituting effectively a bridge between bulk materials and atomic or molecular structures. Nanoparticles having a high surface area-to-volume ratio are generally very reactive, which, on the one hand, may be efficiently exploited by nanotechnology but, on the other hand, may pose serious medical and environmental risks to human populations. The fact that the percentage of constitutive units (atoms, molecules, ions) at the surface is large relative to the total number of such units in the material makes the behavior of nanoparticles in various media very sensitive to topological and energetic heterogeneity of their surface. This is the main reason why the task of establishing the relationship between the surface structure and its reactivity becomes particularly important in the case of nanoparticles.

The intention of this work was to shed more light on surface reactivity of goethite nanoparticles in relation with their surface structure. An important challenge was to test the surface characterization methodology, developed on the basis of advanced molecular-probe methods. The presence, at the surface, of active sites exhibiting different acid strengths, their relative abundance and reactivity towards gaseous molecules were probed with the aid of ammonia adsorption measured by both the two-cycle adsorption method and the flow calorimetry, pyridine pre-adsorption followed

by in-situ Fourier Transform Infrared Spectroscopy in diffuse reflectance mode, together with low-pressure nitrogen and argon adsorption at 77 K coupled with an appropriate modeling approach. Goethite is an iron bearing oxide mineral found mostly in soil, but also in both marine and lake sediments (Schwertmann and Taylor 1989). As this mineral can develop a pH-dependent electric charge in aqueous solutions (Evans et al. 1979; Schwertmann et al. 1985; Hiemstra and Van Riemsdijk 1996; Gaboriaud and Ehrhardt 2003), it has a non-negligible role to play in the control of the transport of toxic and radioactive elements in surface and underground water. The surface charge of goethite particles was found to be mainly dependent on the distribution of various crystalline faces exposed on the material surface (Gaboriaud and Ehrhardt 2003). Among different crystallographic faces forming the surface of a goethite crystal, {101}, {001}, and {121} were by far the most commonly cited ones (Schwertmann and Cornell 1991). For example, the {121} face was shown to grow most rapidly during the formulation of needle-like particles (Cornell and Schwertmann 1996; Weidler et al. 1998).

In a previous work (Prélot et al. 2003), two goethite powdered samples of different particle size were studied thoroughly to obtain a complete image of their morphology and surface heterogeneity by referring to such analytical techniques as high-resolution scanning and transmission electron microscopies, atomic force microscopy, X-ray diffraction, as well as argon and nitrogen sorption experiments. The measurements of low-pressure argon adsorption were subsequently used to model the particle surface as composed of the {001}, {101}, and {121} crystallographic faces. Taking account of all experimental results, it was particularly possible to evaluate the surface areas of these crystallographic faces and their respective proportions. Since the goethite surface can be considered as a polar one, the determination of the acid-base properties and the possible relationships with the distribution of crystallographic faces should be the next step in the surface analysis. Nevertheless, the distributions of polar adsorption sites were not reported before.

The understanding of the adsorption energy distribution for a polar probe on a polar surface is rarely obvious, especially if the conclusions are to be drawn in relation with the particle shape and size. In some special cases, valuable information can be obtained when establishing the relationship between adsorption of selected molecular probes at the solid-gas and solid-liquid interfaces (Michot et al. 1997; Villiéras et al. 1999; Garnier et al. 2007). Adsorption of argon at low temperatures and alcanes at room temperature may be used to derive non-polar adsorption energy distribution. The simultaneous analysis of the adsorption of polar or polarizable probe molecules at the solid-gas and solid-liquid interfaces is exploitable only when both the phenomena lead to similar distribution functions (Villiéras et al. 2002a; Garnier et al. 2007). Nevertheless, it has been recently shown (Prélot et al. 2010) that the image of surface reactivity of amorphous silica may drastically change when passing from the solid–gas to solid–water interface, particularly when the interfacial phenomena are accompanied by the confinement effects. The fact that argon adsorption serves to evaluate non-polar adsorption energy distributions is also utilized to establish the size and shape of such crystalline particles as clay minerals (Villiéras et al. 1997b, 2002b) or goethite (Prélot et al. 2003). When a solid additionally presents some polar surface sites, the overall adsorption energy distribution depends so strongly on the acid-base balance of the adsorbed probe that great differences are observed when applying a non-polar and a polar probe, or two different polar molecules (Villiéras et al. 1999, 2002a, 2002b, 2007).

In the present work, the main emphasis was put on the comparison between two strategies for evaluation of the surface reactivity based on the analysis of acid properties, as scanned with the aid of adsorption at the solid-gas interface. In the first of these strategies, reference was made to ammonia adsorption when measuring adsorption isotherms and the mean enthalpy of adsorption. The second strategy exploited the analysis of the low-pressure adsorption of nitrogen under the conditions of pre-adsorption of pyridine molecules to probe and mask acid surface sites. Two samples of goethite were compared, the commercial one previously studied by Prélot et al. (2003) and a new one containing goethite nanoparticles.

## 2 Experimental section

### 2.1 Materials

Two synthetic goethites ($\alpha$-FeOOH) with an acicular morphology were used. The first sample, Sikovit 10E172, was purchased from BASF (Germany) and further referred to as BASF. Its nitrogen BET specific surface area was 18 $m^2\,g^{-1}$. Main structural and textural features can be found in the previous paper (Prélot et al. 2003).

A laboratory synthetic sample was obtained by a dissolution–crystallization process from 2-line ferrihydrite, a poorly defined highly hydrated phase (Jolivet et al. 2004). 400 mL of an aqueous solution of $Fe(NO_3)_3$(0.1 M) were hydrolyzed by addition of a base solution (NaOH, 1M) at pH 11 and room temperature, leading to a brown precipitate. After ageing for 20 days, the solution was ochre colour and rod-shaped like nanoparticles were obtained. The solid was first separated by centrifugation and then scattered in a solution of perchloric acid (3M) during 2 hours in order to charge the surface positively. Stable aqueous suspensions of

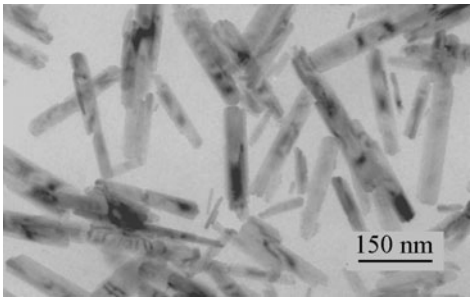


**Fig. 1** TEM images of ECCO goethite

non-aggregated goethite were obtained by repeated centrifugation of this mixture and dispersion in water. Final pH of the colloidal suspension was close to 3.

This sample was further referred to as ECCO. Its nitrogen BET specific surface area was about 65 $m^2\,g^{-1}$. The particles are lath-shaped and can be defined by a thickness, a width, and a length of particles. X-ray scattering pattern gives the apparent mean thickness, $10 \pm 2$ nm for ECCO. The mean particle dimensions deduced from TEM images shown in Fig. 1 are of the order of $70 \pm 20 \times 400 \pm 120$ $nm^2$ for the particle width, and length respectively. The standard deviation of 0.3 that defines the size polydispersity of particles is large for this sample.

### 2.2 Ammonia adsorption at 373 K

Two-cycle adsorption of ammonia at 373 K was measured using a Micromeritics ASAP 2010 Chemi System apparatus (Zajac et al. 2001). Prior to adsorption measurements, a solid sample of ca. 90–180 mg was outgassed for 4 h at 423 K. Then it was cooled down to 373 K in a flow of helium. Successive ammonia doses were sent onto the sample until a final equilibrium pressure of about 40 Torr was reached. The equilibrium pressure was measured after each adsorption step and the amount of $NH_3$ adsorbed was calculated. At the end of the first adsorption cycle, the sample was outgassed under vacuum at 373 K for 60 min to desorb physisorbed molecules and a second adsorption cycle was then performed at the same temperature. It should be noted here that the mass of the solid was optimized so as to obtain sufficiently great adsorption increments between two points of the same isotherm, on the one hand, and to avoid diffusion effects due to high packing density of the nanoparticle sample, on the other hand. The repeatability of the adsorption measurement, estimated from two successive runs with the use of the same solid sample and following the same operating procedure, was within 2% for low-pressure parts of the isotherms and within 12% at higher equilibrium pressures.

A gas-flow calorimetry study of the chemical adsorption of gaseous ammonia at 353 K under dynamic conditions was carried out with the use of a 4Vms Microscal Flow Microcalorimeter equipped with a loop injection facility (a Valco P series valve with a 250 µl injection loop) (Kargol et al. 2005). For this purpose, a solid sample (between 25 and 54 mg) was placed in the calorimetric cell, outgassed at 353 K overnight, and subsequently flushed with a helium flow of 2 $ml\,min^{-1}$ for 4 h. The pulse technique allowed introduction of a defined amount of gaseous ammonia by injection into the carrier gas flowing through the adsorbent bed. Five successive injections of 0.51 µmoles of $NH_3$ were made. Each gas dose was brought into contact with the solid surface, giving rise to a positive heat effect. The evolution of heat was continuously monitored by thermistors sensing temperature changes in the adsorbent bed. Heat evolution ceased after about 15 min and the signal returned to its baseline. Calibration of the areas under the thermal peaks was carried out by dissipating a known amount of energy in the cell under the same flowing conditions (Joule heating using a calibration probe incorporated into the outlet tube) and integrating the related exothermic peak. The molar integral enthalpy of $NH_3$ adsorption, $\Delta_a H_{NH_3}$, was calculated by integrating the area under each peak in the thermal profiles and by dividing it by the amount of $NH_3$ injected into the calorimetric cell. Each experiment was repeated twice and the repeatability of $\Delta_a H_{NH_3}$ determination was within 7%.

### 2.3 Pyridine pre-adsorption at room temperature

Adsorption of pyridine is often used to study the surface acid properties at the solid-gas interface using infrared spectroscopy. Samples with pyridine at the surface were studied by low pressure adsorption of argon and nitrogen to analyze the effect of pyridine adsorption on the surface adsorption distribution of a non polar probe (argon) and a polarizable probe (nitrogen).

Surface heterogeneity at the solid-gas interface was studied before and after pre-adsorption of pyridine on surface acid sites. Samples were first outgassed at 383 K overnight, and then contacted with pyridine vapor at the saturating vapor pressure during 5 hours. After attainment of equilibrium, samples were first outgassed at room temperature during 48–72 hours, down to at least $10^{-5}$ Pa, in order to remove physisorbed pyridine and further analyzed by argon and nitrogen at 77 K in order to analyze the effect of pyridine adsorption on the surface heterogeneity of goethite. A second desorption step was performed by outgassing at 383 K in order to compare with the pristine goethite surface.

Adsorption of pyridine was also followed by in situ Fourier Transform Infrared Spectroscopy in diffuse reflectance mode by using the same outgassing and adsorption procedures. Infrared spectra were recorded using an IFS 55 Bruker Fourier Transform IR spectrometer equipped with a MCT detector (6000–600 $cm^{-1}$) cooled at 77 K and in diffuse reflectance (Harrick attachment) mode.

### 2.4 Low-pressure nitrogen and argon adsorption at 77 K

The experimental procedure for high-resolution and low-pressure gas adsorption (Michot et al. 1990; Villiéras et al. 1997b; Marrocchi et al. 2005) was based on the quasi-equilibrium manometric technique proposed by Grillet and Rouquerol (Grillet et al. 1977; Rouquerol et al. 1988) to enhance the resolution of adsorption isotherms in the low-pressure range, when the first layer of gas is adsorbed on the surface. Low-pressure isotherms of argon and nitrogen at 77 K were recorded on a lab-built automatic quasi-equilibrium manometric set-up (Villiéras et al. 1997b). About 1 g of BASF powder and 0.5 g of ECCO powder were outgassed under a residual pressure of 0.001 Pa at 383 K. A slow, constant, and continuous flow of adsorbate was then introduced into the adsorption cell through a microleak. From the recording of quasi-equilibrium pressure versus time, high-resolution adsorption isotherms were obtained with more than 2000 data points for the filling of the first layer.

Due to the large number of experimental data points acquired by the quasi-equilibrium technique, the experimental derivative of the adsorbed quantity as a function of the logarithm of relative pressure could be calculated accurately. In the present case, iron oxyhydroxide particles were not microporous and multilayer adsorption could be mathematically removed from the experimental adsorption isotherms (Villiéras et al. 1997a). The derivatives thus corresponded to the free energy distribution for the first-layer adsorption and were regarded as fingerprints of interactions for given solid-probe couples. The experimental information was then analyzed using the Derivative Isotherm Summation (DIS) procedure (Villiéras et al. 1992, 1997a, 1997b) to examine the modifications of surface heterogeneity due to pyridine adsorption.

### 2.5 Derivative isotherm summation

The total derivative adsorption isotherm on a heterogeneous surface is modeled by considering two scales of heterogeneity: in the case of crystalline minerals, the surface can be divided into $i$ different crystal faces (patchwise distribution), each face having its own heterogeneity continuously distributed around a mean value (random distribution). The resulting adsorption isotherm can be written as follows:

$$\theta_t = \sum_i X_i \theta_{it} = \sum_i X_i \int_\Omega \theta_i(\varepsilon)\chi_i(\varepsilon)d\varepsilon$$

where $\theta_t$ is the total adsorption isotherm, $\theta_{it}$, the adsorption isotherm on the various energetic domains of the face $i$, $X_i$ is its fractional contribution to $\theta_t$, $\varepsilon$ is the adsorption energy, $\Omega$ is the physical domain of $\varepsilon$, $\theta_i(\varepsilon)$ a "local" theoretical adsorption isotherm and $\chi_i(\varepsilon)$ the dispersion of $\varepsilon$ over the $i$th domain.

In the present study, the local isotherms used to model the first monolayer adsorption were based on the Bragg-Williams-Temkin equation (Villiéras et al. 1992, 1997b). Details about the modeling strategy and parameters for goethite can be found elsewhere (Prélot et al. 2003). The results discussed were as follows: (i) the parameter of apparent lateral interactions ($\omega$), dependent on both the physical lateral interactions between two neighboring adsorbed molecules and the $\chi_i(\varepsilon)$ spreading of normal interactions between the adsorbed molecule and the surface (Villiéras et al. 1997b), (ii) the peak position ($\ln P/P_0$), being a function of the normal and physical lateral interactions of the adsorbed molecule (Villiéras et al. 1992), as well as the monolayer capacity (Vm) for each domain.

As for classical peak fitting techniques, the peak positions and areas depended on the number of peaks chosen for the modeling. The errors in the peak position were lower than 0.1 ($\ln P/P_0$), while those in the monolayer capacity were around 5%.

## 3 Results and discussion

### 3.1 Ammonia adsorption at 373 K

Figure 2 illustrates the measurements of two-cycle ammonia adsorption carried out with the two goethite samples (BASF and ECCO). The approach to calculate the number of acid sites $n_{\text{acid}}$ was based on the following reasoning (Zajac et al. 2001). Linear adsorption parts could be distinguished in both types of adsorption curves at moderate equilibrium pressures, their slopes being almost identical. It was assumed that the linearity of an adsorption isotherm may be ascribed to physical adsorption on non reactive surface. The two straight lines were suitably extrapolated to zero pressure. The difference in the amount adsorbed for points at which the curves reached zero pressure was ascribed to the irreversible chemisorption of basic $NH_3$ at the solid-gas interface and thereby taken as providing estimate of the total number of acid sites at the solid surface per unit mass of the adsorbent. The results of calculation of the number of acid sites are displayed in Table 1. It should be noted that the difference between the two samples is significant only when the results are expressed per unit mass of the adsorbent. The surface site densities normalized with respect to the unit area have similar values for both the solids, then resulting in the comparable numbers of acid sites per sq. nm (2.4 and 2.5 for BASF and ECCO, respectively). Taking into account that the relative error for surface area calculation was about 5%, the maximum absolute uncertainty in determining the real density of acid sites was $\pm 0.2\ \mu\text{mol}\,\text{m}^{-2}$.

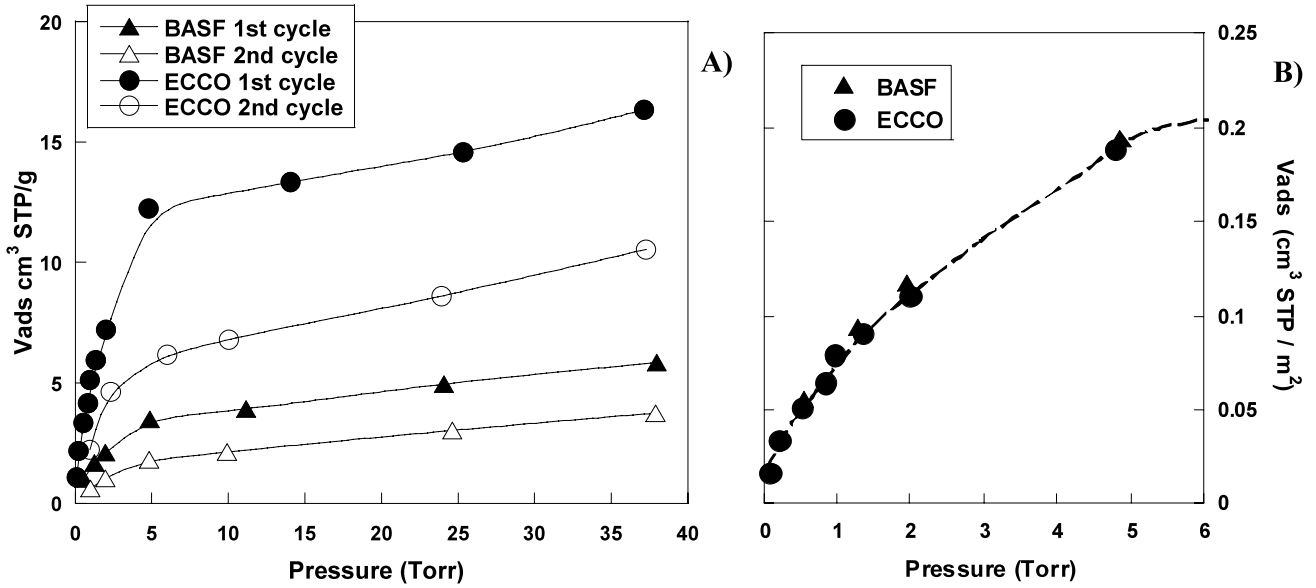


**Fig. 2** (**A**) First-cycle (*solid symbols*) and second-cycle (*open symbols*) adsorption isotherms for gaseous ammonia onto goethite BASF (*triangles*) and goethite ECCO (*circles*), showing the volume of $NH_3$ adsorbed ($V_{ads}$) as a function of the equilibrium pressure at 353 K; (**B**) first-cycle adsorption isotherms showing the volume of $NH_3$ adsorbed per unit surface area. *Solid* and *dashed lines* are drawn to guide to the eye

**Table 1** BET specific surface area, number of acid sites per unit mass or unit area of the adsorbent, and the average acid strength, as measured by two-cycle static adsorption and pulse flow microcalorimetry with the use of ammonia as a molecular probe

| Sample | $S_{BET}$ ($m^2\,g^{-1}$) | $n_{acid}$ ($\mu mol\,g^{-1}$) | $n_{acid}$ ($\mu mol\,m^{-2}$) | Average $\Delta_a H_{NH_3}$ ($kJ\,mol^{-1}$) |
|---|---|---|---|---|
| BASF | $19 \pm 1$ | $75 \pm 3$ | $4.0 \pm 0.2$ | $-45 \pm 2$ |
| ECCO | $65 \pm 2$ | $269 \pm 8$ | $4.2 \pm 0.2$ | $-42 \pm 3$ |

When the data in Fig. 2A are expressed in $cm^3$ STP per unit surface area, the first-cycle curves for both the samples superimpose and yield the same slope in the low-pressure region (cf. Fig. 2B), which means that the affinity between $NH_3$ and the solid surface is equivalent for the two types of goethite. In order to get direct information about the strength of surface acid sites and to shed more light on the solid-adsorbate interaction under dynamic conditions, the integral molar enthalpy of $NH_3$ adsorption, $\Delta_a H_{NH_3}$, was measured by means of the gas-flow calorimetry system operating in the pulse mode. For any injection step, no changes in the signal of the effluent gas percolating through a downstream thermal conductivity detector were registered, indicating that all gas doses were completely retained on the surface. Therefore, the values of $\Delta_a H_{NH_3}$ were determined within the range of chemisorption of $NH_3$ onto all samples studied. Since ECCO and BASF possess very different numbers of acid sites per unit mass, the successive injections of similar $NH_3$ doses in the calorimetry experiment cannot be considered as fully equivalent for both the samples. Different populations of sites should be covered during each injection step since each injection does not correspond to the same proportion of sites (one injection results in $NH_3$ amounts adsorbed of 0.53 and 0.1 $\mu mol\,m^{-2}$ for BASF and ECCO, respectively; this yields respectively 13% and 7% of the total number of acid sites). Instead, the average of the ten enthalpy values was calculated by taking into account the five injections and the two repeated runs (Table 1). In consequence, the average integral enthalpy reported in Table 1 provides information about the mean strength of ammonia-surface interactions giving rise to the irreversible gas adsorption onto a given sample.

The comparison between the average values of $\Delta_a H_{NH_3}$ indicates that the two samples are characterized by acid strengths similar within the experimental error. Taking into account the individual enthalpy effects of successive injections, the BASF goethite gives systematically a little stronger interactions with ammonia. Nevertheless, based only on these results, it is difficult to decide whether the solid surface of the two goethites is homogeneous or just the proportions between weak, moderate and strong acid sites covered by the same amounts of $NH_3$ on both the samples are identical.

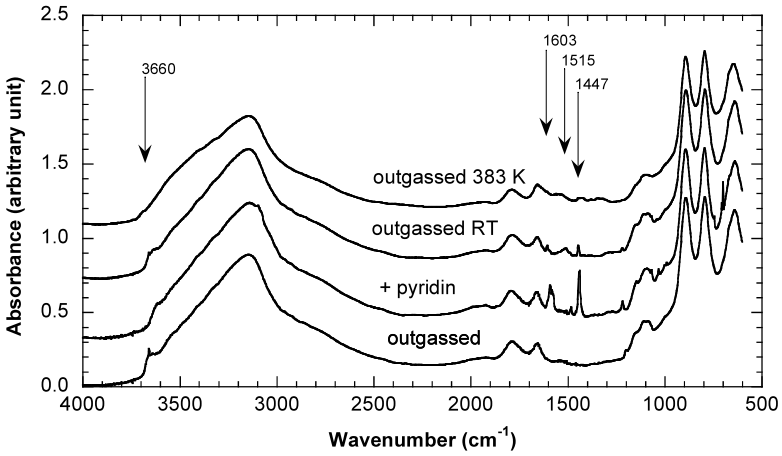


**Fig. 3** Infrared spectra recorded with ECCO goethite outgassed under vacuum, brought into contact with pyridine vapor, and then outgassed either at room temperature (RT) or at 383 K

With these two enthalpy values, it is clear that the 'average' surface acidity of both the samples is rather moderate. The method give global information and nothing can be stated about the presence of Brønsted or Lewis acid sites with various acid strengths.

### 3.2 Pyridine pre-adsorption at room temperature

Commonly, pyridine is considered as being weakly basic and thus capable of interacting preferentially with strong acid sites on the solid surface in the gas phase. The results of infrared (IR) study may be also used to suggest some details as to the site structure or character.

The evolution of infrared spectra of goethite with pyridine adsorption and desorption is illustrated in Fig. 3 for the case of ECCO sample. It can be first observed that pyridine adsorption affects OH intensities lying between 3680 and 3630 $cm^{-1}$ (Morterra et al. 1984a), with a decrease in both the wave number and shoulder intensity. This points toward the specific interactions between the adsorbed molecule and the surface. Specific bands of the adsorbed pyridine can be observed at 1603 and 1447 $cm^{-1}$ and, after outgassing, at 1515 $cm^{-1}$. According to Zaki et al. (2001), no physisorbed pyridine remains on the surface after outgassing. The 1603 and 1447 $cm^{-1}$ bands can be assigned to pyridine interacting with Lewis acid surface sites (Morterra et al. 1984b; Zaki et al. 2001), whereas the 1515 $cm^{-1}$ band is attributed to the formation of pyridinium ions on Brønsted acid sites. As observed by Morterra et al. (1984b), the Brønsted acidity is weak compared to the Lewis-type surface reactivity in the goethite/pyridine system. After outgassing at room temperature, the amounts of pyridine and pyridinium decrease with the concomitant liberation of surface hydroxyls. Most of the previously adsorbed molecules seem desorbed at 383 K, since the specific vibrations of the probe molecule are hardly observed in the IR spectrum. This obviously means that the very strong acid sites are not abundant on the goethite surface, which supports the conclusion drawn on the basis of moderate enthalpy values reported in the previous section. Nevertheless, the distribution functions of surface acid sites are needed to gain more insight into the surface acid-base reactivity.

### 3.3 Argon and nitrogen adsorption at 77 K

Pre-adsorption of an organic at solid-liquid interface prior to surface heterogeneity at solid-gas interface has been successfully used in a previous study (Villiéras et al. 2007). In the present case, pyridine is used as a pre-adsorption probe in order to hide acid surface sites and study its effect on argon and nitrogen adsorption at 77 K.

Adsorption isotherms were obtained for both samples before pyridine adsorption, after pyridine adsorption and evacuation either at room temperature or at 383 K. Figure 4 shows the evolution of the first-layer derivatives of adsorption isotherms for the two goethites. Argon derivative isotherms onto non precovered samples are in agreement with the previous results (Prélot et al. 2003): the main peak is observed at low energy, $\ln(P/P_0)$, around $-4$, with a shoulder at higher energies. In the case of nitrogen, the shape of the derivatives is different, with the main adsorption peak around $-7$ and high amounts adsorbed at a higher energy of about $-14$, evidencing the presence of specific interactions between nitrogen and polar surface sites (Villiéras et al. 1999). It is worth mentioning here that, because of its free electron doublets, molecular nitrogen can be considered as a Lewis base capable of probing the acid Lewis sites on the surface.

In the presence of pyridine, the case of BASF sample is simpler, since the Ar and $N_2$ derivative isotherms decrease in intensity after pyridine adsorption and outgassing at room temperature. When treated at 383 K, the derivatives are superimposed with those of initial samples, indicating that the pyridine molecules are totally desorbed. The differences are more pronounced for ECCO, the amounts adsorbed decreasing strongly for the medium and high-energy adsorption do-

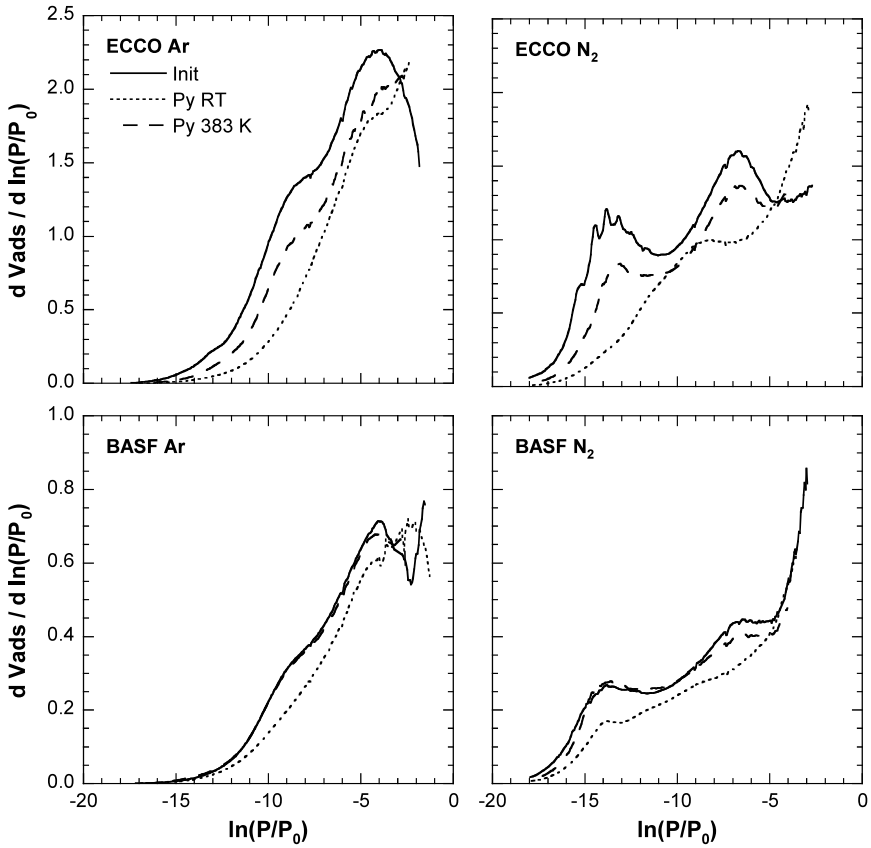


**Fig. 4** Argon and nitrogen derivative adsorption isotherms on goethite outgassed at 383 K (init), after adsorption of pyridine and outgassing at room temperature (Py RT) and at 383 K (Py 383 K)

mains in the case of argon and nitrogen. After outgassing at 383 K, the derivatives are only partially reconstituted, showing that pyridine desorption is not completed in variance with the IR results. For the two samples, it can be concluded that pyridine adsorption affects strongly nitrogen adsorption on high-energy adsorption sites, i.e. polar surface sites, suggesting an acidic character of these sites (Lewis interactions).

The DIS analysis of the argon and nitrogen adsorption isotherms is shown in Fig. 5 for ECCO sample and modeling parameters are collected in Table 2 for the two samples before pyridine adsorption. In this table, argon adsorption domains are assigned to crystallographic faces of goethite according to Prélot et al. (2003), with the low-energy adsorption surfaces assigned to {001} faces, medium-energy adsorption domains corresponding to {101} faces, and the high-energy ones in relation with {121} ends. Based on this assignment, it is possible to evaluate the mean particle length of ECCO particles, following the geometrical model proposed by Prélot et al. (2003): the values obtained ($8 \times 64 \times 364$ nm) are in excellent agreement with the TEM results ($10 \times 70 \times 400$ nm). Nitrogen adsorption domains can be assigned accordingly, except for the high-energy domain corresponding to the adsorption on {121} surfaces and on polar surface sites of the other faces. As is the case for {001} and {101}, {121} should possess surface polar sites. Because of the low {121} specific areas detected by argon, the total amount of nitrogen adsorbed with high-energy values can be considered as a fair estimate of the polar adsorption sites. The calculated amounts of sites are 40 and 180 µmol/g for BASF and ECCO samples, respectively. This corresponds to 1/2 and 2/3 of ammonia sites for BASF and ECCO (Table 1). The plausible explanation may be based on the hypothesis that the gaseous ammonia probes for both the Brønsted and Lewis acid sites, the nitrogen sensing only the Lewis acidity. Nevertheless, further study, with the use of other solids, are necessary to confirm this hypothesis. As can be shown in Table 2, nitrogen adsorption energy for the high-energy sites onto BASF seems slightly higher, i.e., $\ln(P/P_0) = -14.0$, than that for ECCO sample ($\ln(P/P_0) = 13.8$), in agreement with the trend inferred from the calorimetry measurements of ammonia adsorption.

DIS modeling after pyridine adsorption has been carried out using the same adsorption domains and tuning only amounts adsorbed and lateral interaction parameters, following the procedure proposed for silicones grafted on calcium carbonate (Villiéras et al. 2007). In the present case, the distribution of adsorption energy on the pyridine surface is not known and its contribution is to be taken into consideration only for low-energy areas with {001} faces. The results are summarized in Fig. 6, where the amounts

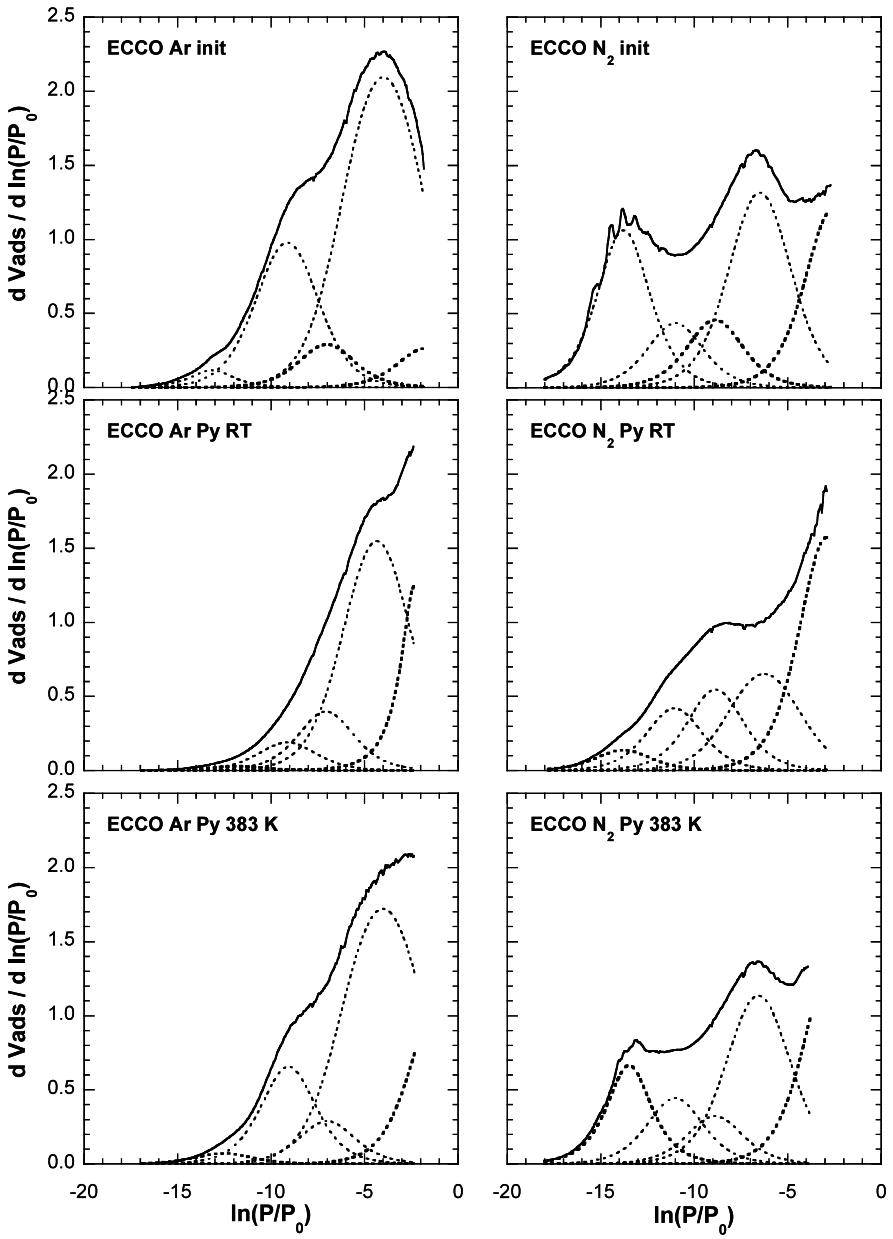


**Fig. 5** DIS modeling of argon and nitrogen derivative isotherms onto goethite outgassed at 383 K (init), after adsorption of pyridine and outgassing at room temperature (Py RT) and at 383 K (Py 383 K): *solid lines*—experimental derivatives, *dotted lines*—local derivatives

adsorbed on the various surface domains are compared. The main information obtained from argon adsorption concerns the {101} faces as, for both the samples, the corresponding specific surface areas decrease when brought in contact with pyridine and further outgassed at room temperature. When outgassing at 383 K, the initial {101} surface area is partially reconstructed for ECCO and totally liberated for BASF. In the case of ECCO goethite, the same behavior is observed for other faces but, after outgassing at 383 K, the {001} surface area is totally freed from pyridine, whereas the {121} domain remains partially covered by pyridine (as observed for {101} faces). Hence these results indicate that the remaining pyridine molecules are mostly located on {101} and {121} surfaces. The analysis is less pertinent in the case of BASF, as the pyridine desorption appears complete in the light of argon adsorption measurements.

The evolution of nitrogen high-energy sites after adsorption and desorption of pyridine is comparable to that for argon adsorption on the {101} domains. This suggests that the high-energy sites are mostly included in such surface domains, as well as are likely present on {121} faces. The roughly constant {101} surface areas for nitrogen are due to possible interactions between nitrogen and pyridine, as was observed in Villiéras et al. (2007) with silicones, thereby increasing the amounts of nitrogen adsorbed in the medium-energy range. It was unfortunately impossible to obtain an experimental reference of nitrogen adsorption on a pyridine monolayer, since physisorbed molecules were desorbed in

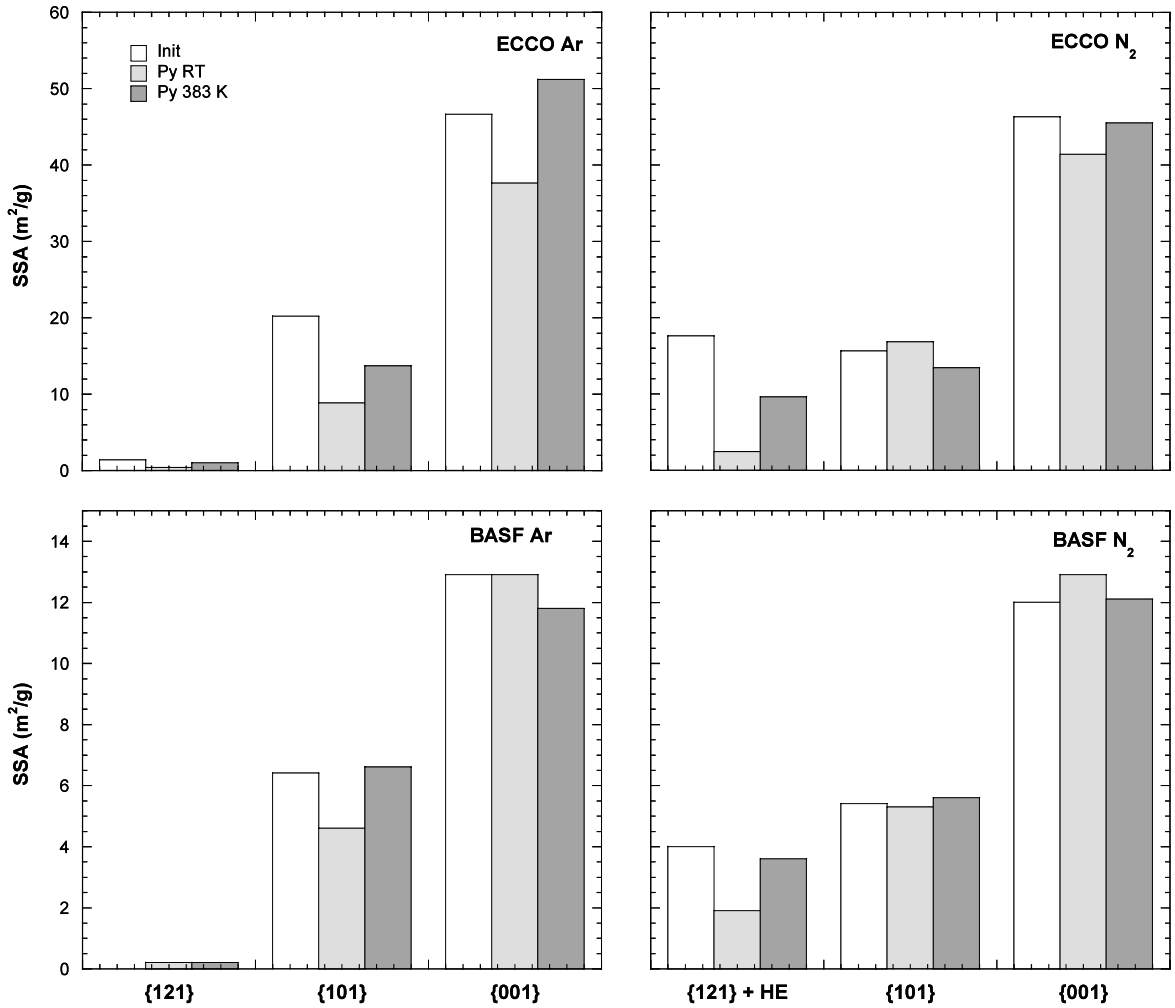


**Fig. 6** Comparison of the amounts adsorbed expressed in terms of the specific surface areas for different faces before and after pyridine adsorption

the outgassing stage performed at room temperature. Another explanation could be that, as pyridine molecules interact with acid surface sites, the remaining nonpolar surface remains roughly constant.

After outgassing at 383 K, 46% and 10% of high-energy sites remain masked by pyridine for the ECCO and BASF samples, respectively. In contrast with the infrared results, nitrogen adsorption makes clear indications for the presence of some remaining pyridine molecules on the surface of the ECCO goethite.

## 4 Conclusion

The main result of the present work was to show the correlation between the surface structure and its reactivity for two types of goethite, a commercial sample and a powered material obtained by a dissolution–crystallization process. The surface reactivity was considered in regard with acid-base interactions between the acid sites located on the various crystallographic faces of goethites and selected basic molecules adsorbed from the gas phase. Concerning the overall acidity, as characterized by the amount of acid sites and the mean strength of ammonia-surface interactions, the two samples possessed similar surface characteristics. The numbers of acid sites per sq. nm were comparable and the affinity between $NH_3$ and the solid surface was equivalent for both the solids. The 'average' surface acidity appeared moderate, as indicated by molar enthalpy values approaching $-40$ kJ mol$^{-1}$. The results of pyridine adsorption coupled with FTIR revealed the presence of both Brønsted and Lewis acid sites. The thermal desorption of pyridine molecules was almost complete at 383 K, indicating that there were few very strong acid sites on the surface of both the samples.

Although the adsorption-based techniques used to date in the present study were not capable of directly suggesting more details as to the acid site structure, it was possi-

**Table 2** DIS modeling parameters for argon and nitrogen adsorption onto initial samples outgassed at 383 K (HE = high energy/polar adsorption sites)

| | $\ln(P/P_0)$ | $\omega$ | Vm ($cm^3/g$) | SSA $m^2/g$ |
|---|---|---|---|---|
| ECCO Ar | | | | |
| {121} | −13.15 | 0.8 | 0.37 | 1.4 |
| {101} | −9.13 | −0.4 | 4.30 | 15.9 |
| {101} | −7.01 | 0.0 | 1.16 | 4.3 |
| {001} | −3.98 | −1.5 | 11.51 | 42.7 |
| {001} | −2.19 | 0.0 | 1.05 | 3.9 |
| | | | total | 68.2 |
| BASF Ar | | | | |
| {121} | −12.33 | 0.4 | 0.03 | 0.1 |
| {101} | −8.76 | −0.6 | 1.17 | 4.3 |
| {101} | −6.57 | 0.4 | 0.55 | 2.0 |
| {001} | −3.93 | −0.1 | 2.46 | 9.1 |
| {001} | −2.10 | 0.0 | 1.01 | 3.7 |
| | | | total | 19.4 |
| ECCO $N_2$ | | | | |
| {121} + HE | −13.77 | 0.2 | 4.03 | 17.6 |
| {101} | −11.00 | 0.0 | 1.74 | 7.6 |
| {101} | −8.87 | 0.0 | 1.83 | 8.0 |
| {001} | −6.46 | −0.4 | 5.79 | 25.3 |
| {001} | −2.52 | 0.0 | 4.80 | 21.0 |
| | | | total | 79.4 |
| BASF $N_2$ | | | | |
| {121} + HE | −14.01 | −0.1 | 0.91 | 4.0 |
| {101} | −11.28 | −0.2 | 0.54 | 2.4 |
| {101} | −8.88 | 0.0 | 0.68 | 3.0 |
| {001} | −6.36 | −0.2 | 1.40 | 6.1 |
| {001} | −3.33 | 0.5 | 1.33 | 5.8 |
| | | | total | 21.3 |

ble to determine the location of such sites on various surface domains. The DIS data treatment applied to argon adsorption resulted in the evaluation of the surface areas of crystallographic faces exposed on the goethite surface and their respective proportions. Argon and nitrogen adsorption experiments supported by the appropriate modeling approach clearly evidenced the presence of polar surface sites characterized by high adsorption energy towards nitrogen. The adsorption measurements, preceded by pyridine preadsorption, confirmed the predominant acidic character of these sites. Such acid sites were found to be located mainly on {121} and {101} faces of particles, though their presence on {001} faces could not be excluded. The amounts of acid sites 'viewed' by nitrogen and ammonia were of the same order of magnitude. Since the results of ammonia adsorption systematically detected more acid sites than those of nitrogen adsorption, the difference was assigned to the presence of Brønsted acid sites interacting selectively with $NH_3$ against $N_2$ in line with the conclusion drawn from the combined pyridine-adsorption and IR study.

Further systematic study based on the strategy of advanced molecular-probe methods, with the use of other model solids combined with spectroscopic characterization, will be necessary to understand the chemical nature of the acid sites on the surface of goethite samples.

**Acknowledgements** The authors greatly acknowledge the financial support of this work by the French ANR within the NANOSurf project (ANR-07-NANO-027).

## References

Cornell, R.M., Schwertmann, U.: The Iron: Structure, Properties, Reactions, Occurrences and Uses, p. 573. VCH, Weinheim (1996)

Evans, T.D., Leal, J.R., Arnold, P.W.: The interfacial electrochemistry of goethite (a-FeOOH) especially the effect of $CO_2$ contamination. J. Electroanal. Chem. **105**, 161–167 (1979)

Gaboriaud, F., Ehrhardt, J.J.: Effects of different crystal faces on the surface charge of colloidal goethite ($\alpha$-FeOOH) particles: an experimental and modeling study. Geochim. Cosmochim. Acta **67**, 967–983 (2003)

Garnier, C., Gorner, T., Villiéras, F., De Donato, P., Polakovic, M., Bersillon, J.L., Michot, L.J.: Activated carbon surface heterogeneity seen by parallel probing by inverse liquid chromatography at the solid/liquid interface and by gas adsorption analysis at the solid/gas interface. Carbon **45**, 240–247 (2007)

Grillet, Y., Rouquerol, F., Rouquerol, J.: Study of physical adsorption of gases by a continuous procedure. 1. Application to determination of specific surface-areas of mesoporous or non-porous adsorbents. J. Chim. Phys. Physico-Chim. Biol. **74**, 179–182 (1977)

Hiemstra, T., Van Riemsdijk, W.H.: A surface structural approach to ion adsorption: the charge distribution model. J. Colloid Interface Sci. **179**, 488–508 (1996)

Jolivet, J.P., Chaneac, C., Tronc, E.: Iron oxide chemistry. From molecular clusters to extended solid networks. Chem. Commun. 481–487 (2004)

Kargol, M., Zajac, J., Jones, D.J., Rozière, J.: Selectivity of gas phase adsorption of propene and propane onto mesoporous silica materials derivatised with Ag(I) and Cu(II) at low surface coverages: comparison between equilibrium adsorption and flow microcalorimetry studies. Thermochim. Acta **434**, 15–21 (2005)

Marrocchi, Y., Razafitianamaharavo, A., Michot, L.J., Marty, B.: Low-pressure adsorption of Ar, Kr, and Xe on carbonaceous materials (kerogen and carbon blacks), ferrihydrite, and montmorillonite: implications for the trapping of noble gases onto meteoritic matter. Geochim. Cosmochim. Acta **69**, 2419–2430 (2005)

Michot, L.J., Didier, F., Villieras, F., Cases, J.M.: Phenol adsorption on activated carbon studied by high resolution argon adsorption and controlled transformation rate thermal analysis. Pol. J. Chem. **71**, 665–678 (1997)

Michot, L., François, M., Cases, J.M.: Surface heterogeneity studied by a quasi-equilibrium gas adsorption procedure. Langmuir **6**, 677–681 (1990)

Morterra, C., Chiorino, A., Borello, E.: An IR spectroscopic characterization of alpha-FeOOH (goethite). Mater. Chem. Phys. **10**, 119–138 (1984a)

Morterra, C., Mirra, C., Borello, E.: IR Spectroscopic study of pyridine adsorption onto alpha-FeOOH (goethite). Mater. Chem. Phys. **10**, 139–154 (1984b)

Prélot, B., Lantenois, S., Nedellec, Y., Lindheimer, M., Douillard, J.-M., Zajac, J.: The difference between the surface reactivity of amorphous silica in the gas and liquid phase due to material porosity. Colloids Surf. A, Physicochem. Eng. Asp. **355**, 67–74 (2010)

Prélot, B., Villiéras, F., Pelletier, M., Gerard, G., Gaboriaud, F., Ehrhardt, J.J., Perrone, J., Fedoroff, M., Jeanjean, J., Lefevre, G., Mazerolles, L., Pastol, J.L., Rouchaud, J.C., Lindecker, C.: Morphology and surface heterogeneities in synthetic goethites. J. Colloid Interface Sci. **261**, 244–254 (2003)

Rouquerol, J., Rouquerol, F., Grillet, Y., Ward, R.J.: In: Hunger, K.K. (ed.) Characterization of Porous Solids, p. 67. Elsevier, Amsterdam (1988)

Schwertmann, U., Cambier, P., Murad, E.: Clays Clay Miner. **33**, 369 (1985)

Schwertmann, U., Cornell, R.M.: Iron Oxides in the Laboratory: Preparation and Characterization, p. 137. VCH, Weinheim (1991)

Schwertmann, U., Taylor, R.M.: In: Dixon, J.B., Weed, S.B. (eds.) Minerals in Soil Environment, pp. 379–438. Soil Science Society of America, Madison (1989)

Villiéras, F., Cases, J.M., François, M., Michot, L.J., Thomas, F.: Texture and surface energetic heterogeneity of solids from modeling of low pressure gas adsorption isotherms. Langmuir **8**, 1789-1795 (1992)

Villiéras, F., Chamerois, M., Bardot, F., Michot, L.J.: Evaluation of wetting properties of powders from low pressure gas adsorption experiments. Contact Angle Wettability Adhes. **2**, 435–447 (2002a)

Villiéras, F., Chamerois, M., Yvon, J., Cases, J.M.: Surface heterogeneity at the solid-gas interface of hydrophilic solids modified by water-repellent molecules. Adsorpt. Sci. Technol. **25**, 561–571 (2007)

Villiéras, F., Michot, L.J., Bardot, F., Cases, J.M., François, M., Rudzinski, W.: An improved derivative isotherm summation method to study surface heterogeneity of clay minerals. Langmuir **13**, 1104–1117 (1997a)

Villiéras, F., Michot, L.J., Bardot, F., Chamerois, M., Eypert-Blaison, C., Francois, M., Gerard, G., Cases, J.-M.: Surface heterogeneity of minerals. C. R. Geosci. **334**, 597–609 (2002b)

Villiéras, F., Michot, L.J., Bernardy, E., Chamerois, M., Legens, C., Gerard, G., Cases, J.M.: Assessment of surface heterogeneity of calcite and apatite: from high resolution gas adsorption to the solid-liquid interface. Colloids Surf. A, Physicochem. Eng. Asp. **146**, 163–174 (1999)

Villiéras, F., Michot, L.J., Cases, J.M., Berend, I., Bardot, F., François, M., Gérard, G., Yvon, J.: Equilibria and Dynamics of Gas Adsorption on Heterogeneous Solid Surfaces. Elsevier, Amsterdam (1997b)

Weidler, P.G., Hug, S.J., Wetche, T.P., Hiemstra, T.: Determination of growth rates of (100) and (110) faces of synthetic goethite by scanning force microscopy. Geochim. Cosmochim. Acta **62**, 3407–3412 (1998)

Ying, J.: Nanostructured Materials. Academic Press, New York (2001)

Zajac, J., Dutartre, R., Jones, D.J., Roziere, J.: Determination of surface acidity of powdered porous materials based on ammonia chemisorption: comparison of flow-microcalorimetry with batch volumetric method and temperature-programmed desorption. Thermochim. Acta **379**, 123–130 (2001)

Zaki, M.I., Hasan, M.A., Al-Sagheer, F.A., Pasupulety, L.: In situ FTIR spectra of pyridine adsorbed on $SiO_2$-$Al_2O_3$, $TiO_2$, $ZrO_2$ and $CeO_2$: general considerations for the identification of acid sites on surfaces of finely divided metal oxides. Colloid Surf. A, Physicochem. Eng. Asp. **190**, 261–274 (2001)